Development of an UWB Rescue Radar System
- Detection of Survivors Using Fuzzy Reasoning -

Iwaki Akiyama
Shonan Institute of Technology
Fujisawa 251-8511 Japan
akiyama@iwaki.org

Masatoshi Enokito
Shonan Institute of Technology
Fujisawa 251-8511 Japan
masa-420@akiyama.elec.shonan-it.ac.jp

Akihisa Ohya
Graduate School of Systems and Information Engineering,
University of Tsukuba
Tsukuba 305-8573 Japan
ohya@cs.tsukuba.ac.jp

Abstract

We are engaged in the development of an ultra-wideband (UWB) rescue radar system for accurately and promptly rescuing survivors buried under collapsed houses in cases of disaster. Since reflected waves from rubble and those from survivors are mixed in the signals received, it is necessary to separate the two to extract the necessary signals. In this study, fuzzy reasoning is used to classify the received signals into the following three classes: components of reflected waves from *survivors*, those from static objects such as *rubble*, and components mainly constituted of other *noise*. In order to examine the target-sensing capability of a radar system incorporating this approach, we carried out experiments with a rubble model targeting subjects. Consequently, the actual position of the subject matched the position where the grade for the survivor class peaked, while the grades for the other classes took small values.

Keywords: rubble, time fluctuation.

1 Introduction

We are engaged in the development of an ultra-wideband (UWB) rescue radar system for accurately and promptly rescuing survivors buried under collapsed houses in cases of disaster[1]. CW radar systems for searching human victims were reported[2]. The radar system now under development is designed to repeatedly transmit wideband pulsed waves in frequency ranges from 3 GHz to 6 GHz into collapsed houses and for searching for survivors in need of help using reception of reflected waves. Since reflected waves from rubble and those from survivors are mixed in the signals received, it is necessary to separate the two to extract the necessary signals. In this study, fuzzy reasoning is used to classify the received signals into the following three classes: components of reflected waves from *survivors in need of help*, those from static objects such as *rubble*, etc., and components mainly constituted of other *noise*. The radar system transmits and receives pulses for approximately 1 minute, and can store received signals in chronological order. Thus, the same delay times of the received signals, that is, temporal variations in reflected components from any object located at a certain distance from the antenna, are used.

This study utilizes, as fuzzy parameters, the following three statistics values for temporal variations: mean value, standard deviation and average frequency obtained from the spectrum. The membership functions for these three parameters were defined and the grades for each class were deduced. For this approach, which we have already proposed for the different application[3], it was decided that the distribution of grades for the three classes in range directions would be displayed without making a final classification. This is because it was assumed that in a real situation in which a *survivor* is sought, an overall decision would be made not only based on the radar system results but on other information as well.

In order to examine the target-sensing capability of a radar system incorporating this approach, we carried out experiments with a rubble model targeting subjects. First, with plywood placed about 1 meter in front of an antenna, one subject stood about 1 meter behind the board. Then, another subject stood further behind the first. We carried out experiments by

setting the distance between the two subjects at 1 m in one experiment and 3 m in another experiment. Then, an antenna was placed about 1 meter above a subject lying face up, and waves were transmitted down and received back. Further, we placed concrete blocks between the antenna and the subject, and checked that the waves transmitted through the rubble, reflected off the subject, and could be received back

We applied our approach to the time-series signals for one minute that were obtained from these experiments, and calculated the grades for the three classes. Consequently, the actual position of the subject matched the position where the grade for the *survivor* class peaked, while the grades for the other classes took small values.

2 UWB Rescue Radar System

As illustrated in Figure 1, the UWB (ultra-wideband) radar system used in this study repeatedly transmits into and receives UWB pulses from rubble, searching for a survivor who is present behind or below it.

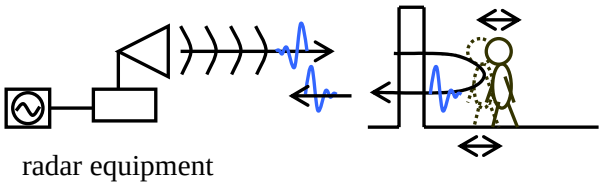

Figure 1: The Basic principle of the searching for survivors using UWB rescue radar system

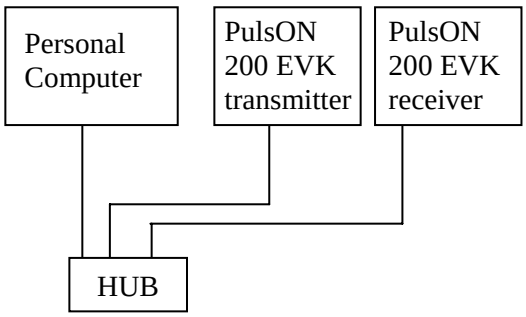

Figure 2: Block diagram of the experimental UWB rescue radar system

Figure 2 is a block diagram of the system that we prototyped in this study. As a transmitter/ receiver, we adopted the PulsON 200 EVK system of Time Domain Corporation in the United States[4]. We installed a horn antenna to this equipment. Both the transmitter and receiver were connected to a personal computer through an Ethernet cable, so the personal computer could control wave transmission and reception. Table 1 lists the specifications of the EVK system.

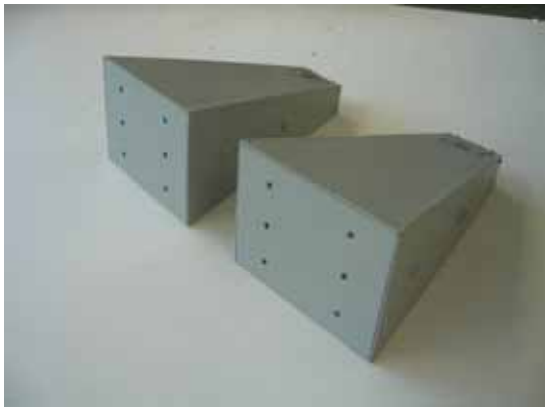

Figure 3: Horn antenna.

Table 1: Specifications of PulsON 200 EVK

Size	Approx. 19.3 × 24.1 × 6.8 cm
Weight	Approx. 750g
Center frequency	Approx. 4.7 GHz
Bandwidth	Approx 3.2GHz
Pulse repetition frequency	Approx. 9.6MHz
Power consumption	Transmission: 12.2 W Reception: 11.9 W
Supply voltage	7.5 VCD

Images were generated by performing envelope detection on received signals and brightness modulation on amplitude, with distance being set in the horizontal direction and the passage of time in the vertical direction. These images are called M-mode images. In such M-mode images, since the waves reflected from static objects do not fluctuate, they are represented as parallel lines, while moving objects are seen as non-parallel line patterns. However, in M-mode images, if the signals received have strong reflection components from a static object, faintly fluctuating components cannot be observed. Thus, in order to remove any reflection components due to

static objects, the $\hat{M}_i$ (t), calculated with the following expression, is displayed as an image [1].

$$\hat{M}_i(t) = \left| \; r_i(t) - \frac{1}{N}\sum_{k=1}^{N} r_k(t) \; \right| \qquad (1)$$

where i is the number of pulse recurrences, t is the time of the received signal, and $r_i(t)$ is the envelope of the *i-th* (ordinal number) received pulse wave.

3 Detection with the Aid of Fuzzy Reasoning of Reflection Components from a Survivor

In order to detect a survivor in need of help using a radar system, the authors have invented an approach using fuzzy reasoning to detect reflection components from survivors. First, the received signals are divided into the following classes: reflection components from *survivors in need of help* (S), reflection components from static objects such as *rubble* (R), and reflection components involving temporal variations in which *noise* (N) is dominant. The characteristics of the *survivors* class are some degree of reception intensity, large temporal variations, and, in particular, strong periodicity. Those of the *rubble* class are high intensity and dominant slow fluctuating components. Those of the *noise* class are low intensity and temporal fluctuations, but no observation of periodicity. The following three parameters are used to quantify the characteristics of each class: the average value (V_m) of temporal fluctuations for one minute at the received voltage, standard deviation (V_{SD}), and the average frequency (f_m) obtained from the spectrum of temporal fluctuations. Figure 4 shows the membership functions for the fuzzy parameters for calculating the grades for each class:

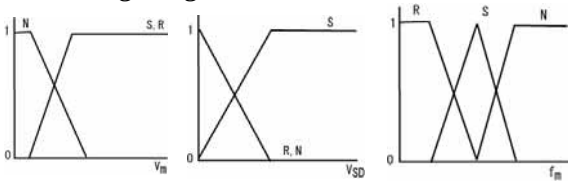

(a) (b) (c)

Figure 4: Membership functions for the three fuzzy parameters; average value (a), Standard deviation (b), and average frequency (c).

From the grades for each class as calculated by the membership functions shown in Figure 4, the corresponding minimum value shall be the grade for that class.

4 Rubble Model Experiment

We construct a rubble model facility to represent a collapsed wooden house. In this rubble model experiment, we carried out a lateral search experiment and a lower search experiment. Figure 5 is a conceptual diagram of these experiments.

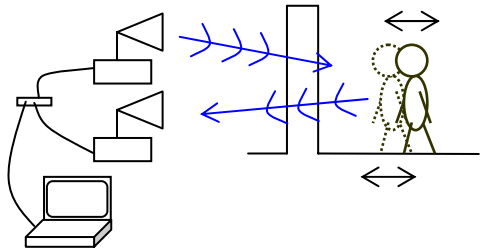

(a) Lateral search experiment

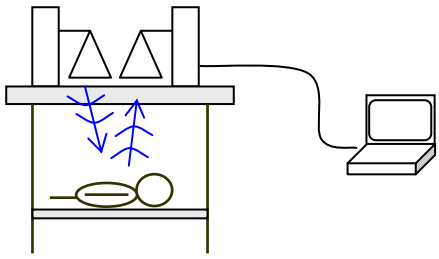

(b) Lower search experiment

Figure 5 Conceptual diagram of rubble model experiment

4.1 Lateral Search Experiment

In the experiment, UWB pulses were transmitted and received by an antenna facing the front of a piece of plywood. We placed the plywood at a position about 1 meter from the antenna. In addition to one subject standing about 1 meter behind the plywood, another subject stood further back at a position diagonal to the first subject. The distance between the two subjects was set to 1 meter in one instance as shown in Figures 6 (a) and 3 meters in another instance as shown in Figures 6 (b). Figure 7 shows the measurements for the signals received in the cases of Figures 6 (a) and (b).

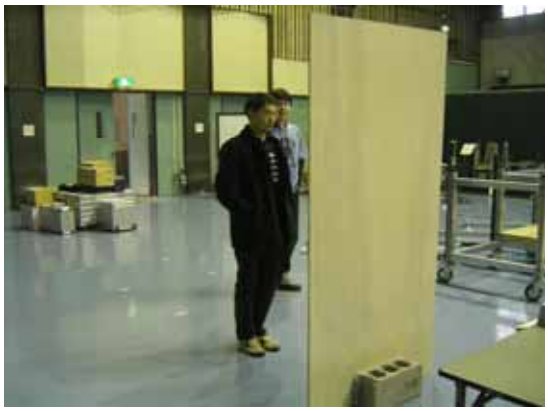

(a) A distance of 1 meter between the two persons

(b) A distance of 3 meters between the two persons

Figure 6 Lateral search experiment.

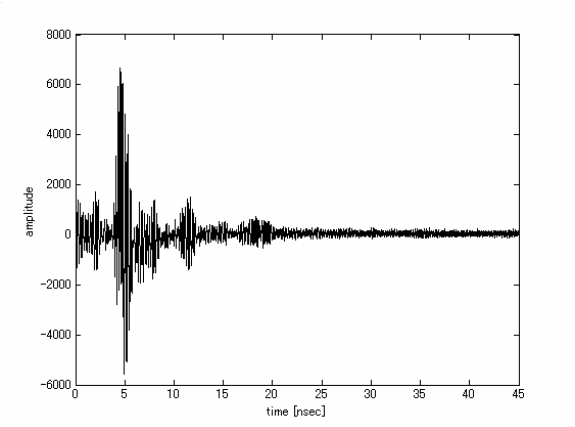

(a) A distance of 1 meter between the two persons

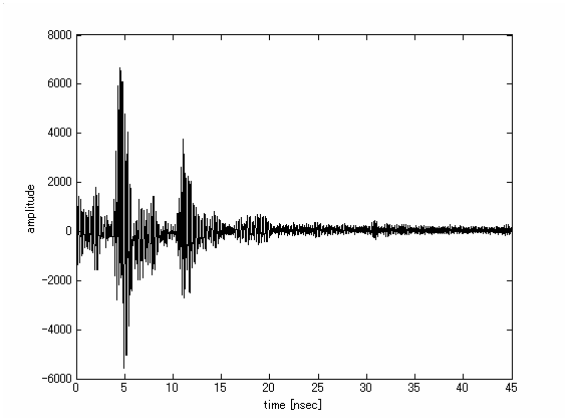

(b) A distance of 3 meters between the two persons

Figure 7 Received Signals

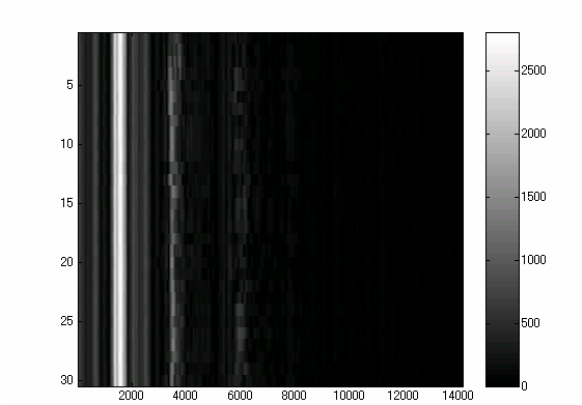

(a) M-mode images.

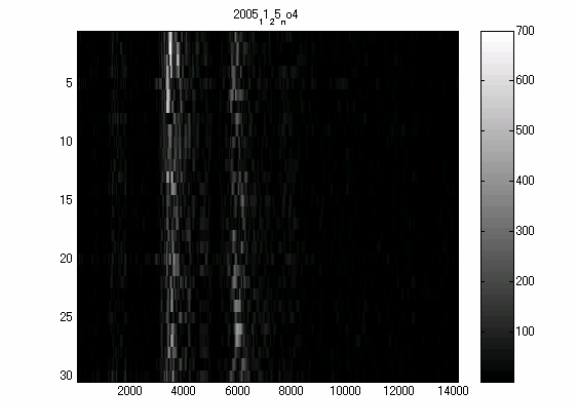

(b) $\hat{M}_i$ (t) images.

Figure 8: M-mode image and $\hat{M}_i$ (t) image when the distance between the two subjects was 1 meter. The distance is expressed along the horizontal direction, and the elapsed time of repeated pulse transmission is expressed along the vertical direction.

Figures 8 and 9 show M-mode images and $\hat{M}_i$ (t) images obtained through envelope detection of received signals that were measured for one minute at 2-second intervals. In the M-mode images, reflections from the plywood were strong and expressed as vertical parallel lines. To the left of those lines, we can see temporal fluctuations corresponding to the subjects. Although we can observe the temporal fluctuations of the subject standing in the back in the $\hat{M}_i$ (t) image of Figure 8 (b), in Figure 9 (b) we cannot detect the back subject when standing 3 meters behind the front subject.

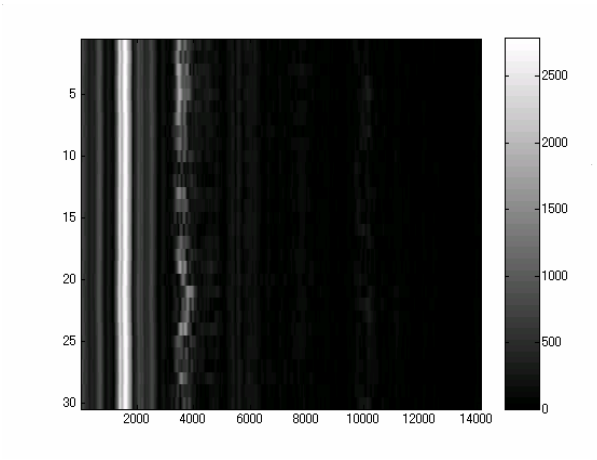

(a) M-mode images

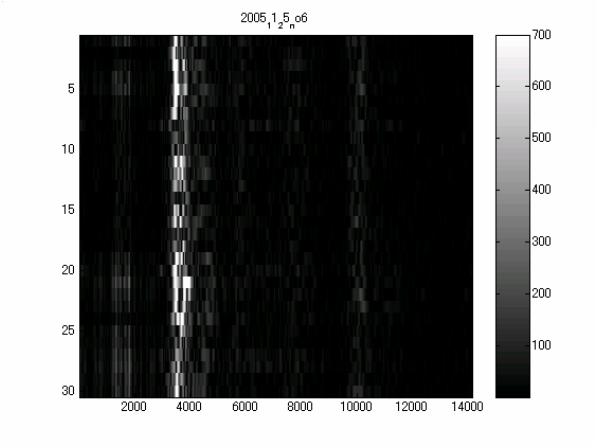

(b) $\hat{M}_i$ (t) images

Figure 9 M-mode image and $\hat{M}_i$ (t) image when the distance between the two subjects was 3 meters. The distance is expressed along the horizontal direction, and the elapsed time of repeated pulse transmission is expressed along the vertical direction.

Figures 10 and 11 show the distributions of the fuzzy parameters V_m, V_{SD}, and f_m in the 1-meter case and the 3-meter case, respectively. As shown in the distribution of V_{SD} (Figure 10(b) and Figure 11(b)), although we can see a peak at the position where the subject was standing, there is also a peak at the location of the plywood, which shows that complete separation from static objects has not yet been realized. Arrows in Figure 10 (b) and Figure 11 (b) indicate the position of the plywood.

Then, Figures 12 and 13 show the determinations of the grades for the classes as obtained using the membership functions: (a) is the distribution of the grades for *survivors*, (b) the distribution of the grades for *rubble*, and (c) the distribution of the grades for *noise*. The distribution of the minimum values of the grades obtained from the distributions of (a), (b) and (c) are shown by (d) and thus represent the final grades for the three classes.

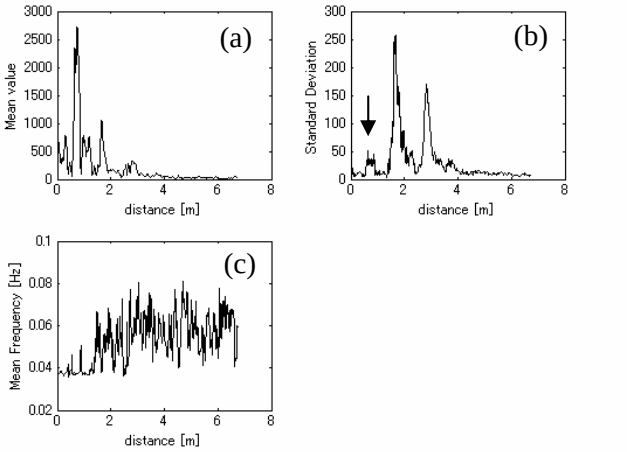

Figure 10: Distribution of Fuzzy Parameters: In the 1-meter Case. (a) is V_m,, (b) V_{SD}, and (c) f_m.

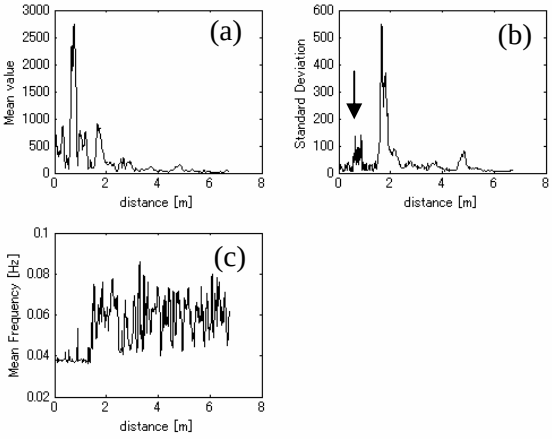

Figure 11: Distribution of fuzzy Parameters: In the 3-meter Case. (a) is V_m,, (b) V_{SD}, and (c) f_m.

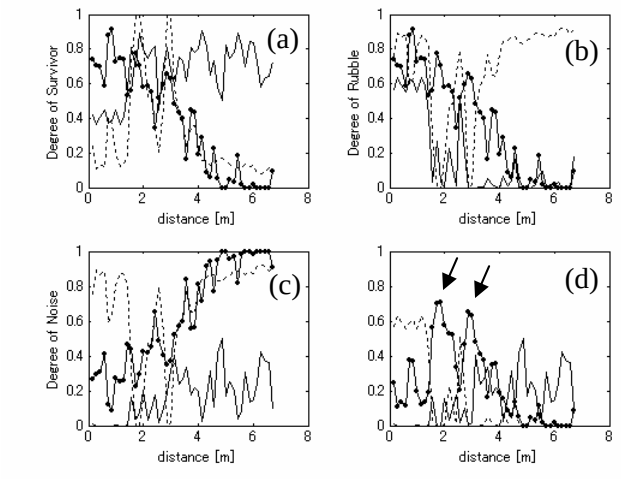

Figure 12: Distribution of grades for each class as determined by the membership functions in the 1-meter case. (a) is for *survivors*, (b) for *rubble*, and (c) for *noise*. V_m is expressed as solid line, V_{SD} as dotted line, and f_m as dash-dot line. (d) is the distribution of the minimum values obtained from the each distributions of grades. The distribution of grades for *survivors* is expressed as dash-dot line, for *rubbles* as dotted line, and for *noise* as solid line.

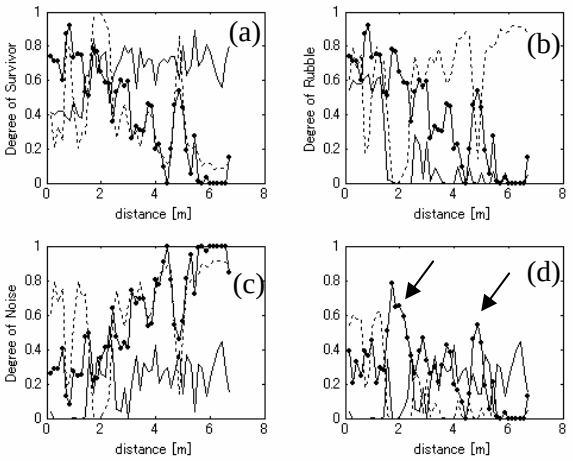

Figure 13: Distribution of grades for each class as determined by the membership functions in the 3-meter case. (a) is for *survivors*, (b) for *rubble*, (c) for noise. V_m is expressed as solid line, V_{SD} as dotted line, and f_m as dash-dot line. (d) is the distribution of the minimum values obtained from the each distributions of grades. The distribution of grades for *survivors* is expressed as dash-dot line, for *rubbles* as dotted line, and for *noise* as solid line

As shown in Figure 12 (d), we notice that in the grade for *survivors* in need help, peaks can be seen at the 2-meter position and the 3-meter position as shown by arrows. In contrast, the grades for the other classes are small. This shows that it is most likely that one survivor each exists at the 2-meter position and the 3-meter position, which matches the positions where the subjects were actually standing. As shown in Figure 13 (d), we notice that in the *survivor* grade, there are peaks at the 3-meter position, 4-meter position and 5-meter position, in addition to the 2-meter position. However, at the 3-meter and 4-meter positions, the *noise* grade is also high, which shows that it is most likely that survivors are present at the 2-meter and 5-meter positions as shown by arrows, matching the positions where subjects were actually standing.

4.2 Lower Search Experiment

We conducted a lower search experiment assuming the case of a person buried under a collapsed house. We installed an antenna unit downward, with a subject lying underneath. Figure 14 is a photograph showing how the experiment was conducted.

Figure 15 shows M-mode images and $\hat{M}_i(t)$ images. There were strong reflections from the block and we were unable to observe reflections from the subject who was beneath it. Figure 16 shows the distributions of the fuzzy parameters. Looking at the distribution for V_{SD}, we cannot find a clear peak attributable to the subject because reflections from the block are so strong.

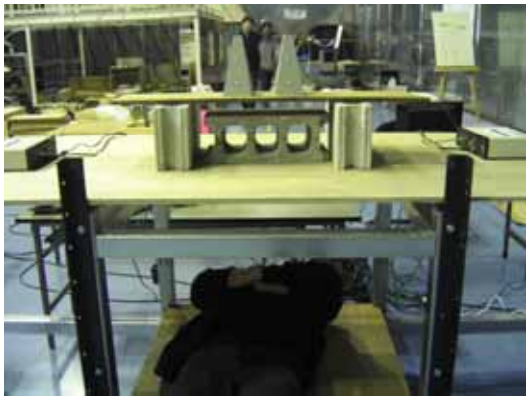

Figure 14: Lower Search Experiment

Figures 17 (a), (b) and (c) show the grades for each class, and Figure 17 (d) is the plot of the minimum values of the grades. Figure 17 (d) shows that in the *survivor* grade, there is a peak

at the 1.5-meter position as shown by an arrow. This position matches the actual position of the subject.

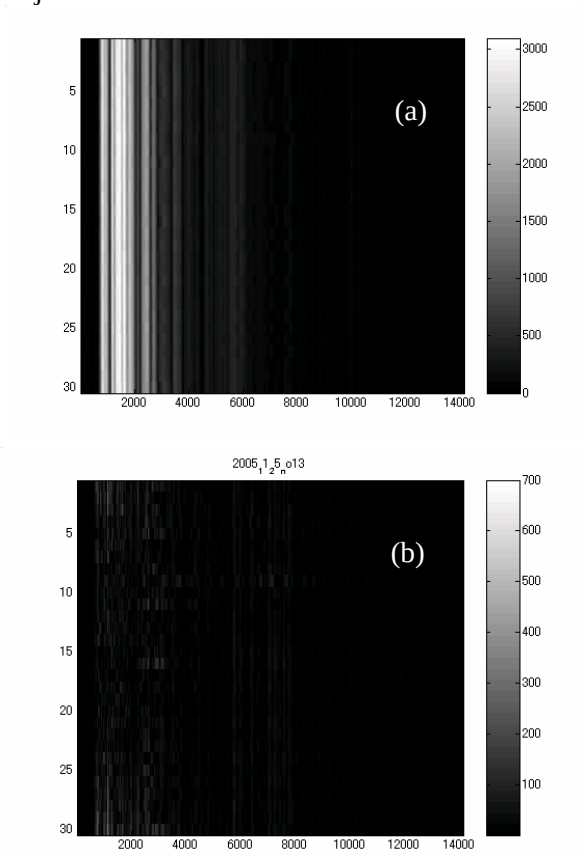

Figure 15: M-Mode Image (a) and $M_i(t)$ image (b) .

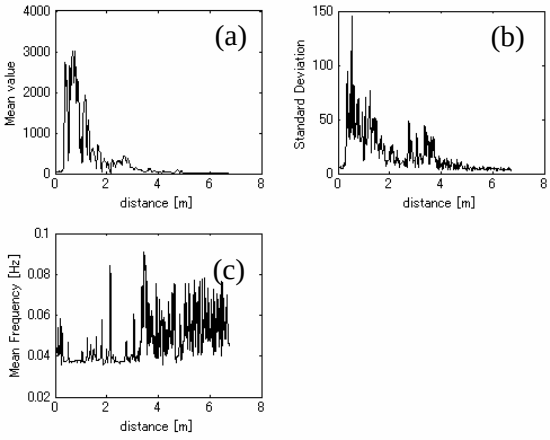

Figure 16: Distribution of fuzzy parameters. (a) is V_m,, (b) V_{SD}, and (c) f_m.

Figures 18 to 20 show the results for the case in which the subject took a deep breath in the experiment shown in Figure 14. Figure 18 shows the M-mode image and $\hat{M}_i(t)$ image.

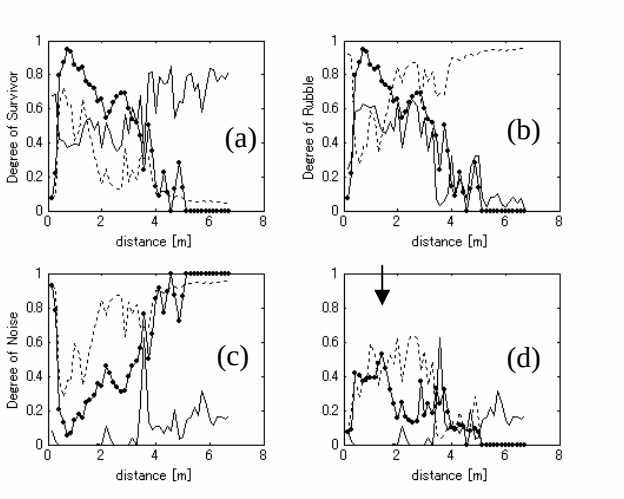

Figure 17: Distribution of grades for each class as determined by the membership functions. (a) is for *survivors*, (b) for *rubble*, (c) for *noise*. V_m is expressed as solid line, V_{SD} as dotted line, and f_m as dash-dot line. (d) is the distribution of the minimum values obtained from the each distributions of grades. The distribution of grades for *survivors* is expressed as dash-dot line, for rubbles as dotted line, and for *noise* as solid line.

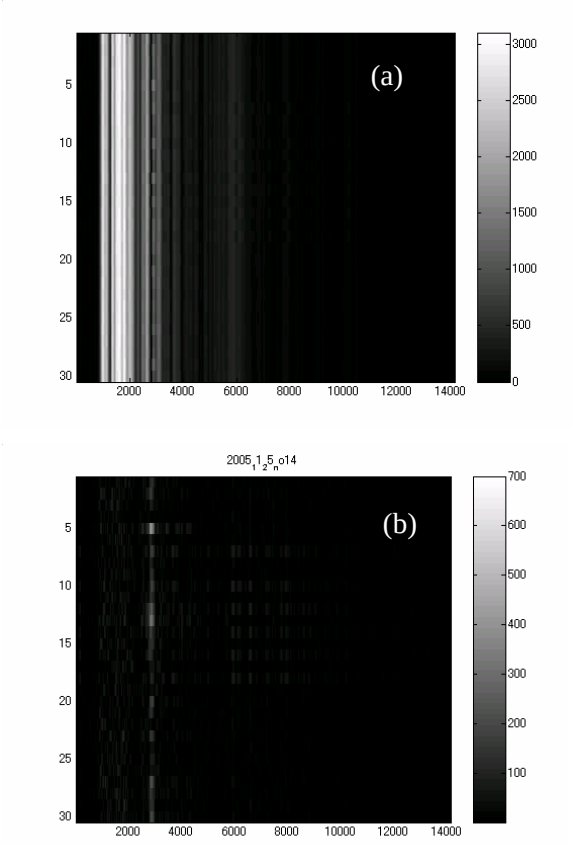

Figure 18: M-Mode Image (a) and $\hat{M}_i(t)$ Image (b).

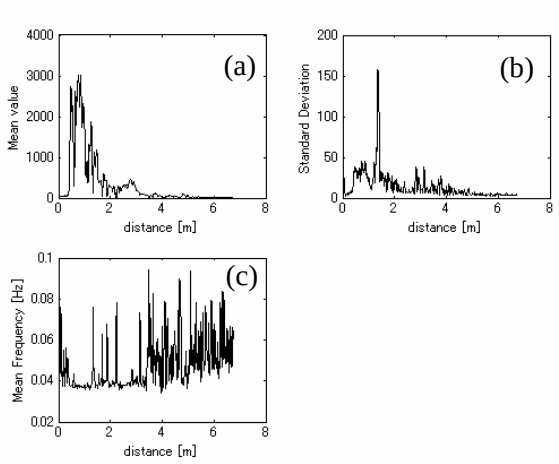

Figure 19: Distribution of fuzzy parameters. (a) is V_m,, (b) V_{SD}, and (c) f_m.

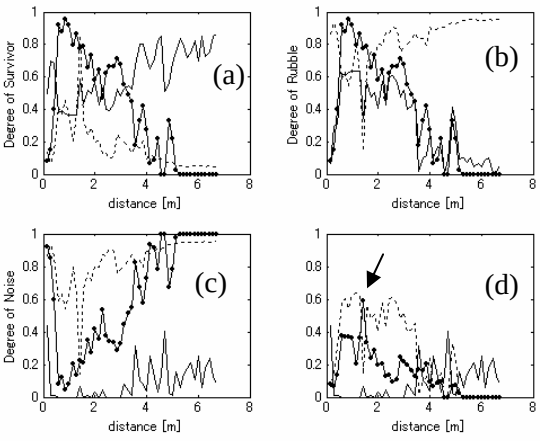

Figure 20: Distributions of Grades for Each Class. (a) is for *survivors*, (b) for *rubble*, (c) for *noise*. V_m is expressed as solid line, V_{SD} as dotted line, and f_m as dash-dot line. (d) is the distribution of the minimum values obtained from the each distributions of grades. The distribution of grades for *survivors* is expressed as dash-dot line, for *rubbles* as dotted line, and for *noise* as solid line.

Figure 19 shows the distributions of the fuzzy parameters, and Figure 20 shows the distributions of the grades for each class. In the $\hat{M}_i(t)$ image of Figure 18 (b), we can see temporal fluctuations at the position where the subject was lying.

Among the fuzzy parameters shown in Figure 19, the V_{SD} value is high. As shown in Figure 20 (b), we see a peak grade value for the *survivor* class at about the 1-meter position as shown by an arrow. This position matches the actual position of the subject.

5 Conclusion

With the aid of received signals using the fuzzy reasoning of a UWB rescue radar system, we established an approach to separate reflection components of rubble and other obstructions and extracted the reflection components of persons posing as *survivors*. Using this approach, we conducted rubble model experiments and examined the target-sensing capability of the radar system. As a result, we were able to successfully distinguish a subject standing 1 meter behind plywood and another subject standing 3 meters as well as 1 meter behind the first subject.

When we applied this approach in conditions in which a subject lying on his back was breathing quietly as well as breathing deeply, we succeeded to detect the position of the subject.

Acknowledgements

We conducted part of this study with assistance from the Special Project for Earthquake Disaster Mitigation in Urban Areas of the Ministry of Education, Culture, Sports, Science and Technology.

References

[1] I. Akiyama, Y. Araki, M. Isozaki, M. Ohki, A. Ohya (2004): UWB Radar System Sensing of Human Being Buried in Rubbles for Earthquake Disaster, *Abstract of EUROEM2004*, 163-164, July 2004.

[2] K-M.Chen, Y.Huang, J. Zhang and A.Norman: Microwave life-detection systems for searching human subjects under earthquake rubble or behind barrier, IEEE Trans. on Biomedical Engineering, Vol.27, No.1, 105-114, 2000.

[3] I.Akiyama, Y.Kawahara, G.Ohashi, K.Omoto, K.Itoh, X.Cheng, and A.Ohya (2000) Diagnostic system for screening of breast cancer using the most trained neural network and partially trained neural network, *Proceedings of the conference IPMU'2000*, volume 1, pages 13-18, Madrid, Spain July 2000.

[4] http://www.timedomain.com/Files/products/P200EVK.pdf